FOREX Publication
Open Access | Rapid and quality publishing

International Journal of
Electrical and Electronics Research (IJEER)
Research Article | Volume 11, Issue 1 | Pages 202-212 | e-ISSN: 2347-470X

PV Integrated UPQC with Intelligent Control Techniques for Power Quality Enhancement

Ramesh Rudraram[1*], Sasi Chinnathambi[2] and Manikandan Mani[3]
[1,2]*Department of EEE, Annamalai University, India*
[3]*Department of EEE, Jyothishmathi Institute of Technology and Science, Karimnagar, Telangana, India*

***Correspondence:** Ramesh Rudraram; rameshrudraeee@gmail.com

ABSTRACT- The configuration and control of a Unified Power Quality Conditioner (UPQC) coupled with Photovoltaic (PV) system is proposed in this work. By integrating PV to UPQC, the twin advantages of decarbonized clean energy generation in addition to enhanced Power Quality (PQ) is obtained. The series and shunt compensators, which together constitute the UPQC are sequentially interfaced to the common dc-link. In addition to infusing active PV generated power, the UPQC shunt compensator diminishes the load side power quality concerns. The role of a series compensator is to ensure that both the load and source voltages are in-phase perfectly. The PV system is integrated to the UPQC through a DC/DC Interleaved Cuk-converter and by regulating the duty cycle of the Interleaved Cuk-converter, utmost possible power is derived from the PV using Crow Search Algorithm (CSA) assisted Perturb and Observation (P&O) Maximum Power Point Tracking (MPPT) technique. The designed hybrid MPPT technique is capable of operating at Maximum Power Point (MPP) under both Partial Shading Condition (PSC) and uniform insolation condition. A d-q theory-based control is employed with the assistance of Proportional Integral (PI) controller for controlling the working of UPQC. The dynamic working of the PV based UPQC is evaluated on the basis of simulation outcomes attained from MATLAB.

Keywords: PV-UPQC, PQ, series compensator, d-q theory, shunt compensator, Interleaved Cuk-converter, CSA assisted P&O MPPT.

ARTICLE INFORMATION

Author(s): Ramesh Rudraram, Sasi Chinnathambi and Manikandan Mani;

Received: 29/01/2023; **Accepted**: 28/03/2023; **Published**: 30/03/2023;
e-ISSN: 2347-470X;
Paper Id: IJEER 2901-02;
Citation: 10.37391/IJEER.110128
Webpage-link:
www.ijeer.forexjournal.co.in/archive/volume-11/ijeer-110128.html

1. INTRODUCTION

The ubiquity of sensitive power electronic loads like switched mode power supplies, computers, variable speed drives, and others have expanded with the evolution of semiconductor technology. In spite of being highly efficient, these loads have the unfavourable property of drawing nonlinear currents, owing to which considerable distortions in voltage arise at the point of common coupling in case of distributed power systems [1].Additionally, there is a growing focus on the production of clean energy through rooftop PV system installations in both commercial and small apartment buildings [2, 3].However, on the other hand grid voltage fluctuation occurs as a consequence of the intermittent nature of the PV and their increased infusion leads to grid instability. Furthermore, several PQ issues such as flickering, interruptions, sags/swells etc., develops on the grid side. These issues, which influence the voltage quality, have detrimental impact over the sensitive power electronic devices interfaced to the network, consequently leading to severe economic losses [4, 5].

So, for improving the PQ of the distributed power system, several custom power devices like Dynamic Voltage Resonator (DVR) [6, 7], Distribution Static Compensator (DSTATCOM) [8, 9] and UPQC [10, 11] are employed. The DVR secures the load from breakdown or tripping by curtailing significant PQ issues such as sags/swell, harmonics, flickers and interruptions but on the downside, they are not effective in balancing voltage sags of high magnitude [12]. The DSTATCOM is comparatively better at delivering the required reactive power injection for enhancing the system reliability and moreover, it is exceptional in dealing with situations like abrupt load removals and non-linear working conditions. The operation of DSTATCOM, however is affected by significant amount of power losses if the load voltage reference value is 1.0 p.u. [13]. The DVR is able to provide series compensation, while the DSTATCOM is able to provide shunt compensation. The UPQC is capable of providing both series and shunt compensation and it is also effective in delivering overall PQ enhancement for both grid current and load voltage.

The limitation associated with the intermittency of the PV system is overcome by employing a significant MPPT technique in conjunction to a DC-DC converter. The former regulates the duty cycle of the latter for maximizing the magnitude of power derived from the PV array [14]. The boost converter is frequently employed for improving the output voltage of the PV module but it not efficient in high gain applications, due to large amount of conduction losses and switching losses. The buck-boot converter, which is effective

FOREX Publication
Open Access | Rapid and quality publishing
International Journal of Electrical and Electronics Research (IJEER)
Research Article | Volume 11, Issue 1 | Pages 202-212 | e-ISSN: 2347-470X

for both step-up and step-down voltage conversion is affected by the limitation of irregular input current owing to which, it is unable to maintain its operating point around MPP. The Cuk-converter has continuous input current and it comes from the buck-boost converter family but the presence of large amount of input current ripples affects its MPPT operation. So, an Interleaved Cuk-converter, which is effective in curbing current ripples in addition to having continuous input and output current is selected in this work for improving the PV output module voltage [15, 16]. The choice of an appropriate MPPT technique is instrumental in heightening the PV system efficiency. The conventional MPPT techniques of Perturbation and Observation (P&O), Hill-Climbing (HC) and Incremental Conductance (IC) display exceptional performance under uniform insolation but they are rather in effective under PSC. Several metaheuristic algorithms such as Particle Swarm Optimization (PSO) [17], Cuckoo Search (CS) [18], Genetic Algorithm (GA) [19], etc. are effective under PSC but they are hindered by limitations such as large tuning parameters and structural complexity. Thereby, a hybrid MPPT approach obtained by combining both P&O and CSA [20] is proposed for guaranteeing optimal MPPT operation under both uniform insolation and PSC.

A PV fed UPQC, which supports both decarbonized power generation in addition to enhanced PQ is proposed in this work. The non-linear nature of the PV system is overcome by implementing Interleaved Cuk-converter with CSA assisted P&O MPPT. The control of the series and shunt compensators of UPQC is established by the application of d-q theory. The dynamic nature of the presented PV-UPQC is analysed according to the simulation results acquired from MATLAB.

2. PROPOSED SYSTEM DESCRIPTION

The expanded influx of power electronic loads in the distribution system, has to lead to the existence of numerous PQ issues. Therefore, with the aim of subduing these PQ issues in addition to promoting the generation of clean energy, a configuration of PV fed UPQC is designed in this paper as seen in *figure 1*. The interfacing of the PV to the UPQC is achieved by the employment of an Interleaved Cuk-converter. The choice of an Interleaved Cuk-converter is due to its continuous input and output current along with its remarkable ability to reduce current ripples. For aiding the extraction of maximum power, a novel CSA assisted P&O MPPT, which is successful under both uniform insolation and PSC is proposed.

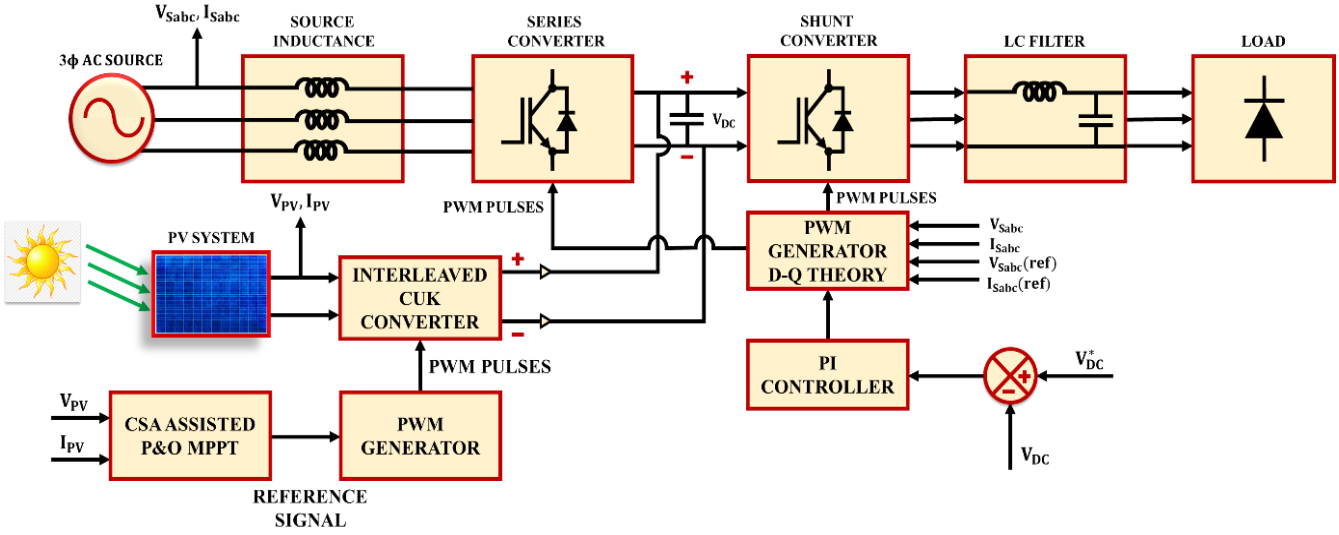

Figure 1: Proposed PV integrated UPQC configuration

The output voltage and current of the PV module (I_{PV}, V_{PV}) is provided as input to the hybrid MPPT and the required change in duty ratio command is obtained as output. The PWM generator receives this output signal and governs the working of the converter by generation of gating pulses. The controlled output of desired voltage level, acquired from the converter is fed to the DC link. The PI controller along with the d-q theory is used for controlling the working of the series and shunt compensators of the UPQC. The actual and reference DC-link voltages (V_{DC}, V^*_{DC}) are compared and the estimated error is given for processing to the PI controller. The reference current signal is generated on the basis of d-q theory, by considering the source current and source voltage ($I_{sabc} V_{sabc}$) along with the reference current and reference voltage ($I_{sabc(ref)}, V_{sabc(ref)}$).

In accordance to the reference current and the control signal from PI controller, the PWM generator produces pulses for controlling the working of the series and shunt compensators. Thus, the PQ of the both the grid current and load voltage is improved.

3. PROPOSED SYSTEM MODELLING

3.1 Modelling of PV System

The modelling of each PV cells, which together constitute the PV module, is based on single-diode model as given in *figure 2*. This model encompasses a current source coupled parallel to a diode (D) and a resistance (R_{sh}) in addition to another resistance (R_S), which is linked in series.

FOREX Publication
Open Access | Rapid and quality publishing
International Journal of Electrical and Electronics Research (IJEER)
Research Article | Volume 11, Issue 1 | Pages 202-212 | e-ISSN: 2347-470X

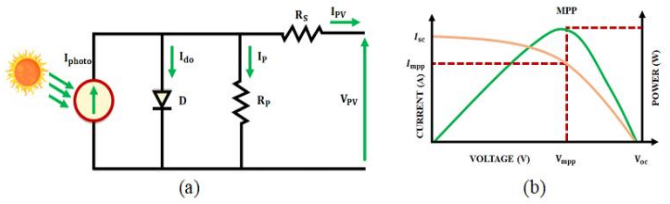

Figure 2: PV cell (a) single diode equivalent circuit and (b) Characteristic curve

The current derived from the PV cell is expressed as,

$$I_{PV} = I_{ph} - I_d - I_{sh} \quad (1)$$

Where, the photocurrent is indicated using the term I_{ph}, the diode current and the current flowing across R_{sh} is indicated using the terms I_d and I_{sh} respectively. On replacing I_d and I_{sh} with appropriate expressions, *eq.* (1) becomes,

$$I_{PV,C} = I_{ph} - I_o\left[exp\left(\frac{Q(V_{PV,C}+I_{PV,C}R_S)}{\eta k T_c}\right) - 1\right] - \frac{V_{PV,C}+I_{PV,C}R_S}{R_{sh}} \quad (2)$$

Where, the reverse saturation or leakage current is denoted as I_o, the output current derived from a single cell is denoted as $I_{PV,C}$, the cell output voltage is denoted as $V_{PV,C}$, the cell temperature is denoted as T_c, the Boltzmann's constant is denoted as$k$, the electron charge and the ideality factor of the diode is denoted using the terms Q and η respectively. The output current from a module is given as,

$$I_{PV,M} = I_{ph} - I_o\left[exp\left(\frac{Q(V_{PV,M}+N_S I_{PV,M}R_S)}{N_S \eta k T_c}\right) - 1\right] - \frac{V_{PV,M}+N_S I_{PV,M}R_S}{N_S R_{sh}} \quad (3)$$

Where, the number of PV cells linked in series to form a module is represented using the term N_s. The PV modules are connected in parallel or/and series combination to give the PV array, so the *eq. (3)* is modified as,

$$I_{PV,M} = I_{ph}N_p - I_o N_p\left[exp\left(\frac{Q\left(V_{PV,M}+\frac{N_S}{N_p}I_{PV,M}R_S\right)}{N_S \eta k T_c}\right) - 1\right] - \frac{V_{PV,M}+\frac{N_S}{N_p}I_{PV,M}R_S}{\frac{N_S}{N_p}(R_{sh})} \quad (4)$$

Where, the number of parallel linked cell strings are specified using the term N_p. The PV cell characteristic curve is given in *figure 2 (b)*. The cell temperature and solar irradiance$G$ have a significant influence over the photo current,

$$I_{ph} = (I_{ph,n} + K_1 \Delta T_c)\frac{G}{G_n} \quad (5)$$

Where, the solar irradiance at Standard Test Condition (STC) is specified as G_n, while the photocurrent at STC is specified as $I_{ph,n}$. The change in cell temperature is specified using the term ΔT_c. The diode saturation current is given as,

$$I_o = I_{o,n}\left(\frac{T_c}{T_{c,n}}\right)^3 exp\left[\frac{Q(E_{go})}{\eta k}\left(\frac{1}{T_{c,n}} - \frac{1}{T_c}\right)\right] \quad (6)$$

Where, the materials energy band gap is denoted as E_{go}. At STC, the diode saturation current is given as,

$$I_{o,n} = I_{ph,n} exp\left[\frac{Q(V_{OC,n})}{N_S \eta k T_c}\right] \quad (7)$$

By the effective management of the slope of current and voltage relationship, the performance of the cell is enhanced by both the series and shunt resistance.

$$R_{sh} > \frac{10V_{oc}}{I_{SC}} \quad (8)$$

$$R_s > \frac{0.1V_{oc}}{I_{SC}} \quad (9)$$

Where, the terms I_{SC} and V_{oc} represent the short circuit current and the open circuit voltage respectively. The CSA assisted P&O MPPT algorithm, improves the efficiency of the PV by regulating the duty cycle of Interleaved Cuk-converter.

3.2 Modelling of Interleaved CUK Converter

The Interleaved Cuk-converter comes with the exceptional capability to minimize the distortions in its input in addition to having an excellent transient performance and enhanced efficiency. The circuit topology of the interleaved Cuk converter entails two switches, four inductors and capacitors, two diodes in addition to one load resistor as seen in *figure 3 (a)* and its four distinct operational modes are represented as,

Mode 1($t_o - t_1$): During this mode ($t_o - t_1$), the switch S_1 is in ON state, while the other switch S_2 is in OFF state as seen in *figure3 (b)*. The inductor L_1 is in the state of charging, whereas the inductor L_2 is in the state of discharging. The capacitor C_1 discharges and supplies to the load. The ripple current is given as,

$$\Delta I_{L_1} = \left(\frac{t_1 - t_o}{L_1}\right)(V_{PV} - R_1 i_{L_1}) \quad (10)$$

$$\Delta I_{L_2} = \left(\frac{t_1 - t_o}{L_2}\right)(V_{PV} - V_{C_2} - (R_2 + R_4) i_{L_2}) \quad (11)$$

On considering,$L_1 = L_2 = L_a$,$R_1 = R_2$ and$i_{L_1} = i_{L_2}$ then

$$\Delta I_1 = \Delta I_{L_1} - \Delta I_{L_2} = \left(V_{C_2} + R_4 i_{L_2}\right)\left(\frac{t_1 - t_o}{L_a}\right) \quad (12)$$

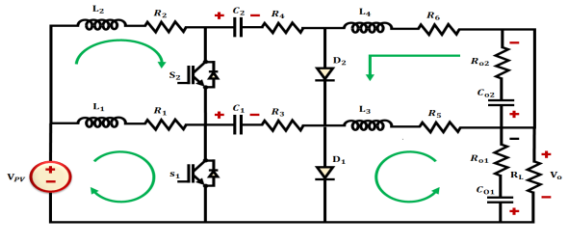

(a)

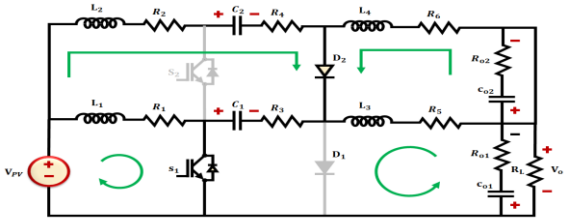

(b)

FOREX Publication
Open Access | Rapid and quality publishing
International Journal of Electrical and Electronics Research (IJEER)
Research Article | Volume 11, Issue 1 | Pages 202-212 | e-ISSN: 2347-470X

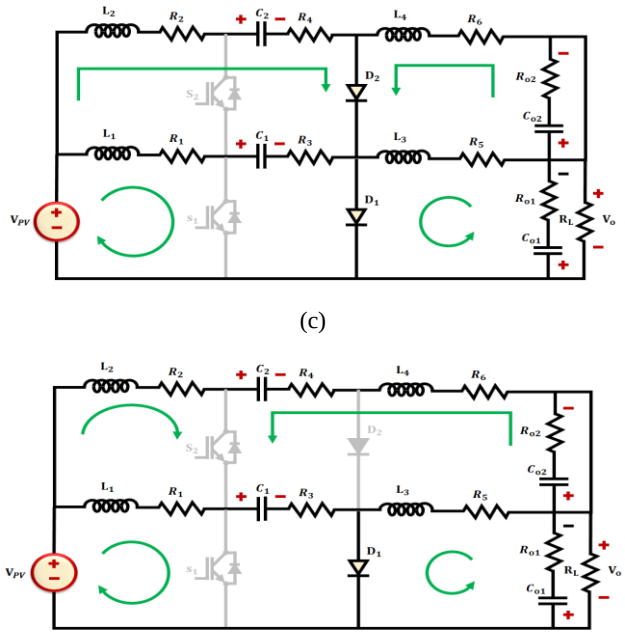

(c)

(d)

Figure 3: Interleaved Cuk converter (a) Circuit (b) Mode 1 (c) Mode 2 and (d) Mode 3

Mode 2($t_1 - t_2$): As seen in *figure 3 (c)*, both the switches are turned OFF during this mode. The capacitors C_1 and C_2 are charged by the energy discharged from inductors L_1 and L_2respectively. The discharged energy from inductors L_3 and L_4 is transferred to the load. The ripple current is given as,

$$\Delta I_{L_1} = \left(\frac{t_2 - t_1}{L_1}\right)(V_{PV} - V_{C_1} - (R_1 + R_3) i_{L_1}) \quad (13)$$

$$\Delta I_{L_2} = \left(\frac{t_2 - t_1}{L_2}\right)(V_{PV} - V_{C_2} - (R_2 + R_4) i_{L_2}) \quad (14)$$

On considering, $L_1 = L_2, V_{C_1} = V_{C_2}$, $R_1 = R_2$ *and* $R_3 = R_4$,

$$\Delta I_2 = \Delta I_{L_1} - \Delta I_{L_2} = 0 \quad (15)$$

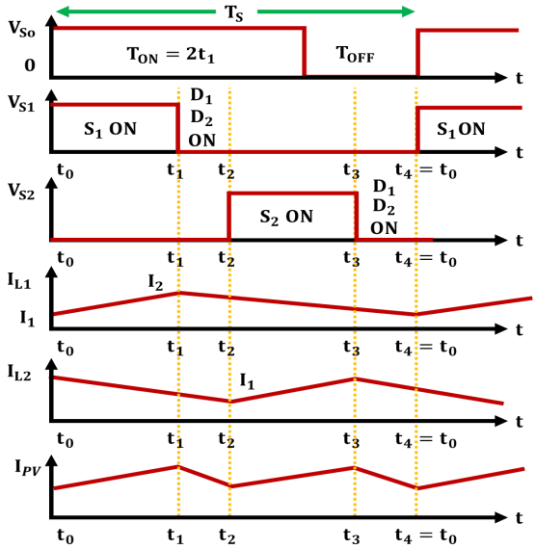

Figure 4: Interleaved Cuk converter operational waveform

Mode 3($t_2 - t_3$): In this mode, the switch S_2 is turned ON and the switch S_1 is turned OFF as illustrated in *figure 3 (d)*. Unlike Mode 1, the inductor L_2 is in the state of charging, whereas the inductor L_1 is in the state of discharging during Mode 3. The capacitors C_1 is charged by the energy transferred from inductors L_1. Here, the energy from capacitor C_2 furnishes the load and *figure 4* displays the operational waveform of the Interleaved Cuk-converter. The ripple current is given as,

$$\Delta I_{L_1} = \left(\frac{t_3 - t_2}{L_1}\right)(V_{PV} - V_{C_1} - (R_1 + R_3) i_{L_1}) \quad (16)$$

$$\Delta I_{L_2} = \left(\frac{t_3 - t_2}{L_2}\right)(V_{PV} - R_2 i_{L_1}) \quad (17)$$

On considering, $L_1 = L_2 = L_a, R_1 = R_2$ *and* $i_{L_1} = i_{L_2}$, then

$$\Delta I_3 = \Delta I_{L_1} - \Delta I_{L_2} = (-V_{C_1} - R_3 * i_{L_1})\left(\frac{t_3 - t_2}{L_a}\right) \quad (18)$$

Mode 4($t_3 - t_4$): This mode is similar to mode 2, since the switches are in OFF state. However, during this mode, the cancellation of ripple current takes place,

$$\Delta I_4 = \Delta I_{L_1} - \Delta I_{L_2} \quad (19)$$

The voltage across capacitor C_1 is given as,

$$V_{C_1} = V_{PV} + V_{o1} \quad (20)$$

For switch S_1, the volt-sec balance is given as,

$$\frac{V_{PV} D T_S}{2} + (V_{PV} - V_{C_1})(1 - D)\frac{T_S}{2} \quad (21)$$

By substitution of *eq. (20) in eq. (21)*,

$$V_{o1} = -\frac{V_{PV} D}{(1 - D)} \quad (22)$$

Where the duty cycle is specified using the term$D$. The duty cycle of Interleaved Cuk converter is varied with the intention of ensuring maximum transfer of power using the CSA assisted P&O MPPT.

3.3 Modelling of CSA Assisted P&O MPPT

The P&O, which is a prominent MPPT technique is known for its simple algorithm and ease of implementation. Moreover, it identifies the MPP on the basis of trial-and-error method. In this method, the value of current and voltage are studied periodically for evaluating the PV power. Then on the basis of the variance in power value, the converter's duty cycle is perturbed. The MPP position as seen in *figure 5* is obtained according to the following equations,

$$\frac{dP_{PV}}{dV_{PV}} = 0 = MPP \quad (23)$$

$$\frac{dP_{PV}}{dV_{PV}} > 0 = Left\ side\ of\ MPP \quad (24)$$

$$\frac{dP_{PV}}{dV_{PV}} < 0 = Right\ side\ of\ MPP \quad (25)$$

FOREX Publication
Open Access | Rapid and quality publishing
International Journal of Electrical and Electronics Research (IJEER)
Research Article | Volume 11, Issue 1 | Pages 202-212 | e-ISSN: 2347-470X

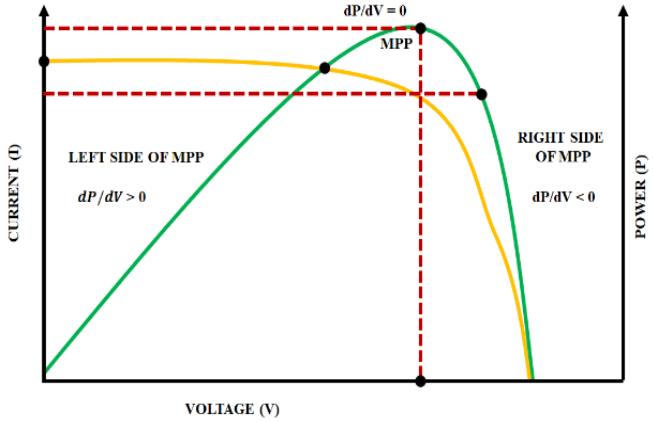

Figure 5: Operating principle of a PV panel

The value of $\frac{dP_{PV}}{dV_{PV}}$ is positive on the curve's left side, while it is negative on the curve's right side. For a positive power variance, the operating voltage is incremented, whereas, for a negative power variance, the operating voltage is decremented in order to reach the MPP. However, this technique is less efficient under PSC.

The CSA, which is a bio-inspired population-based metaheuristic optimization algorithm displays excellent performance under PSC. Its design is mainly based on the characteristic trait of a crow to conceal and procure food. Moreover, the crow also keeps an eye on other crows for uncovering the location of their concealed food.

On the flip side, if the tracked crow becomes aware that it is being followed, it alters its position to deceive other crows. Consider two crows, crow i and crow j, among which the former is the tracker and the latter is the one being tracked. According to the value of Awareness Probability (AP), two states are considered for updating the position of the crows, which are:

State 1: $\boldsymbol{r \geq AP}$**:** In this state, the crow j is ignorant and clueless about being followed and its food location is approached by crow i on the basis of the subsequent equation,

$$x_i^{iter+1} = x_i^{iter} + r \times fl \times (m_j^{iter} - x_i^{iter}) \quad (26)$$

Where, an arbitrary number between [0 1] is specified as r and the flight length is specified using the term fl. At iteration $(iter + 1)$, the crow i's position is specified as x_i^{iter+1} and at iteration $(iter)$, the memory vector of crow j is specified as m_j^{iter}.

State 2: $\boldsymbol{r < AP}$**:** In this state, the crow j is fully aware of being followed and it misleads crow i by shifting to an arbitrary location in the search space. The crow i's position is given as,

$$x_i^{iter+1} = a\ random\ location \quad (27)$$

The crow's smart movements in search space are displayed in *figure 6*. At each iteration, according the current and prior fitness values of every vector, the values of x_i^{iter} and m_j^{iter} are updated. In case of applying CSA as MPPT, the power P_{PV} is considered as the fitness, while the crow i's position x_i is considered as duty cycle D_i.

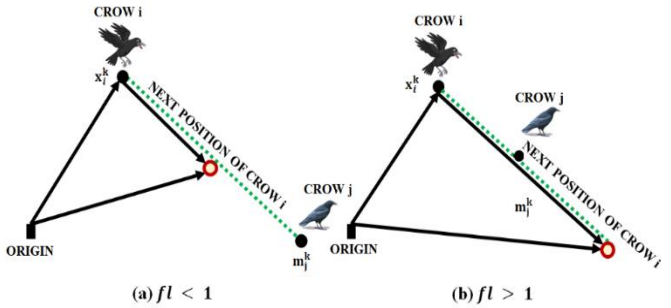

Figure 6: Movements of crow during the process of foraging for food

The steps followed while implementing CSA as MPPT is given below,

1. Initialize tuning parameters of CSA, memory of crows and duty cycle.
2. At initial iteration, for determining the current optimal solution D_{best}^0, the value of initial objective function P_i^0 is evaluated.
3. A new solution D_i^{k+1} is generated.

In case of *state 1*, the new duty cycle is given as,

$$D_i^{k+1} = D_i^k + r \times fl \times (m_j^k - D_i^k) \quad (28)$$

Where, the duty cycle at $k + 1$ iteration is represented as D_i^{k+1}. In case of *state 2*, the new duty cycle is given as,

$$D_i^{k+1} = a\ random\ duty\ cycle \quad (29)$$

Both the above cases are generally summarized as,

$$D_i^{k+1} = \begin{cases} D_i^k + r \times fl \times \left(m_j^k - D_i^k\right), & \text{if r} \geq \text{AP} \\ a\ random\ duty\ cycle\ , \quad otherwise \end{cases} \quad (30)$$

4. The new fitness P_i^{k+1} is evaluated and the new duty cycle D_i^{k+1} is updated.

The feasibility relation for the acceptance of the computed fitness values is given as,

$$P_i^{k+1}(D_i^{k+1}) > P_i^k(D_i^k) \quad (31)$$

5. In the flock, every crow's memory vector m_i^{k+1} is updated.
6. The termination criterion $(iter = iter_{max})$ is checked.

FOREX Publication
Open Access | Rapid and quality publishing
International Journal of Electrical and Electronics Research (IJEER)
Research Article | Volume 11, Issue 1 | Pages 202-212 | e-ISSN: 2347-470X

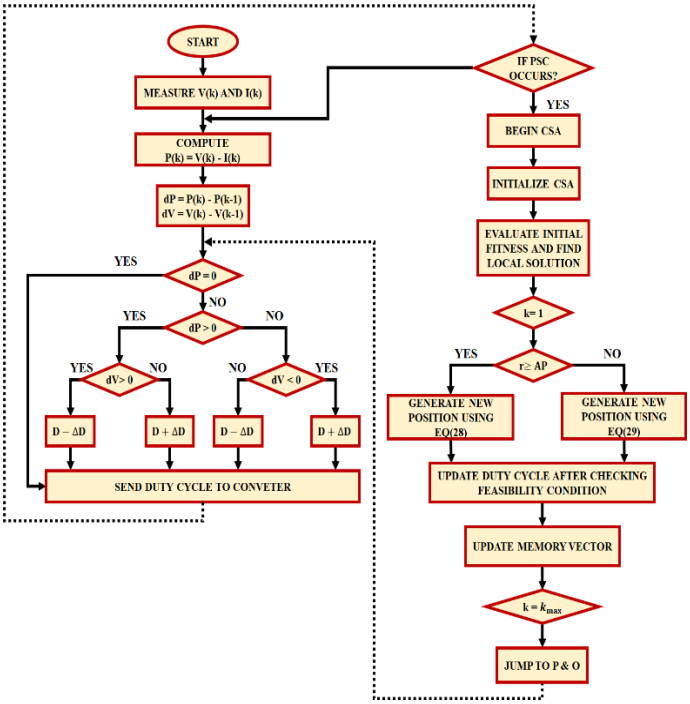

Figure 7: Flowchart of Hybrid CSA assisted P&O MPPT

A hybrid algorithm is proposed by combining both P&O and CSA for obtaining effective MPPT operation in both PSC and uniform shading conditions. The flowchart of the proposed CSA assisted P&O is given in *figure 7*. Under uniform insolation, the MPP is tracked by applying the P&O technique and under PSC, the hybrid algorithm is employed for tracking the MPP. The MPPT process is initially carried out using CSA and after obtaining the global best position, the process is continued with P&O. By the fusion of both these approaches, the operation of the MPPT is strengthened further at non-linear operating conditions.

3.4 Control of UPQC

The UPQC, which is an excellent power conditioning device capable of both shunt and series compensation, is effective in delivering overall PQ enhancement by improving both grid voltage and load current. The shunt compensator has the ability to subdue the PQ issues like reactive power and harmonics on the load side through injection of current. The series compensator possesses the ability to eliminate the sag/swell issues on the grid side by injecting appropriate out-phase or in-phase voltage. A DQ theory-based control, which is a time domain technique, is chosen due to its good dynamic response and reduced computational complexity.

3.4.1 Shunt Compensator Control approach

The shunt compensator aims to significantly minimize the PQ issues including reactive power, neutral current and current harmonics on the load side. Furthermore, the active PV power is also infused by the shunt compensator. Its overall control approach is given in *figure 8*. The generation of reference current, which has unity power factor in addition to being sinusoidal in nature, is essential for shunt compensator, since it operates in indirect control mode. The regulation of the DC-bus voltage to a desired value is done by employing a PI controller. The transformation of the load current to d-q rotating frame is carried out initially.

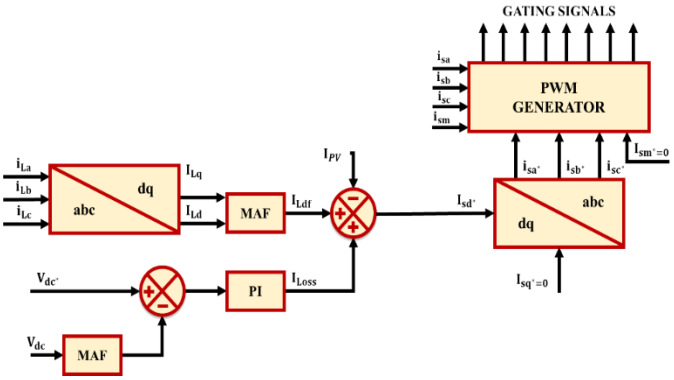

Figure 8: Control structure for shunt compensator

A Moving Average Filter (MAF) is employed for filtering the I_d component to obtain I_{Ldf} and its transfer function is given as,

$$G_{MAF}(z) = \frac{1}{M}\frac{1-z^{-M}}{1-z^{-1}} \quad (32)$$

Where,

$$M = \frac{T_w}{T_s} \quad (33)$$

Where, the sampling time and averaging window is specified as T_s and T_w respectively. The d-axis reference grid current is given as,

$$I_{sd}^{*} = I_{Ldf} + I_{loss} - I_{PV} \quad (34)$$

Where, the term I_{Ldf} specifies the synchronous frame active load current, the term I_{loss} specifies the current equivalent of the loss component. The value of the reference grid current in q-axis is zero. The currents $(i_{sa}^{*}, i_{sb}^{*}, i_{sc}^{*})$ are obtained after conversion of the d-q domain reference grid current to *abc* domain. By analogizing the actual and reference grid currents, an error signal is generated, which is then provided to the PWM generator for generating suitable pulses.

3.4.2 Series Compensator Control approach

The series compensator ensures that the load voltage and source voltage are perfectly in-phase by injecting the required out of phase or in-phase voltage. Its control structure is given in *figure 9*.

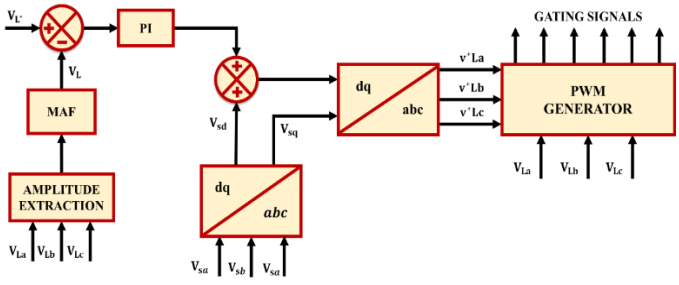

Figure 9: Control structure for Series compensator

FOREX Publication
Open Access | Rapid and quality publishing
International Journal of Electrical and Electronics Research (IJEER)
Research Article | Volume 11, Issue 1 | Pages 202-212 | e-ISSN: 2347-470X

The grid voltage in abc domain is transformed to *d-q* domain and the magnitude of load voltage is given as,

$$V_L = \sqrt{\frac{2}{3}}(V_{La}^2 + V_{Lb}^2 + V_{Lc}^2) \quad (35)$$

The ripple contents in the obtained load voltage are filtered. The actual and reference load voltages are compared and the estimated error is supplied to the PI controller. The PI controller output is added to the grid voltage d-axis component for obtaining the load voltage d-axis component. The load voltage q-axis component is similar to V_{sq} . The reference signals $(v_{La}^*, v_{Lb}^*, v_{Lc}^*)$ are obtained after conversion of the d-q domain reference load voltages to *abc* domain. By analogizing the actual load voltage and the reference load voltage, the PWM generator produces gating pulses for the series compensator.

4. RESULTS AND DISCUSSION

The necessity for improved PQ has garnered immense attention due to the rising prevalence of sensitive loads in the distributed power system. Hence, the configuration of a PV-UPQC with suitable control approaches for enhancing the PQ is presented in this paper. The PV system entails Interleaved Cuk-converter and CSA assisted P&O MPPT for deriving maximum power in all operating conditions. Moreover, the UPQC is controlled using *d-q* theory and PI controller. *Table 1* gives the parameter specifications of the presented PV-UPQC.

Table 1: Parameter Specifications

Parameters	Specifications
PV panel	
Power	$10kW$
Number of panels	$500W, 20\ panels$
V_{OC},I_{SC}	$22.6V, 41.6A$
V_{SC}	12V
Interleaved Cuk converter	
Inductors L_1, L_2, L_3, L_4	$4.2mH$
Capacitors C_1, C_2	$22.6\ \mu F$
CapacitorsC_{01}, C_{02}	$2200\mu F$
Switching frequency	$10kHz$
Switch	IGBT
Non-Linear load	
Resistance	100Ω
Inductance	$10mH$
AC Source	
Voltage	$330 - 470V$
Current	0-30A

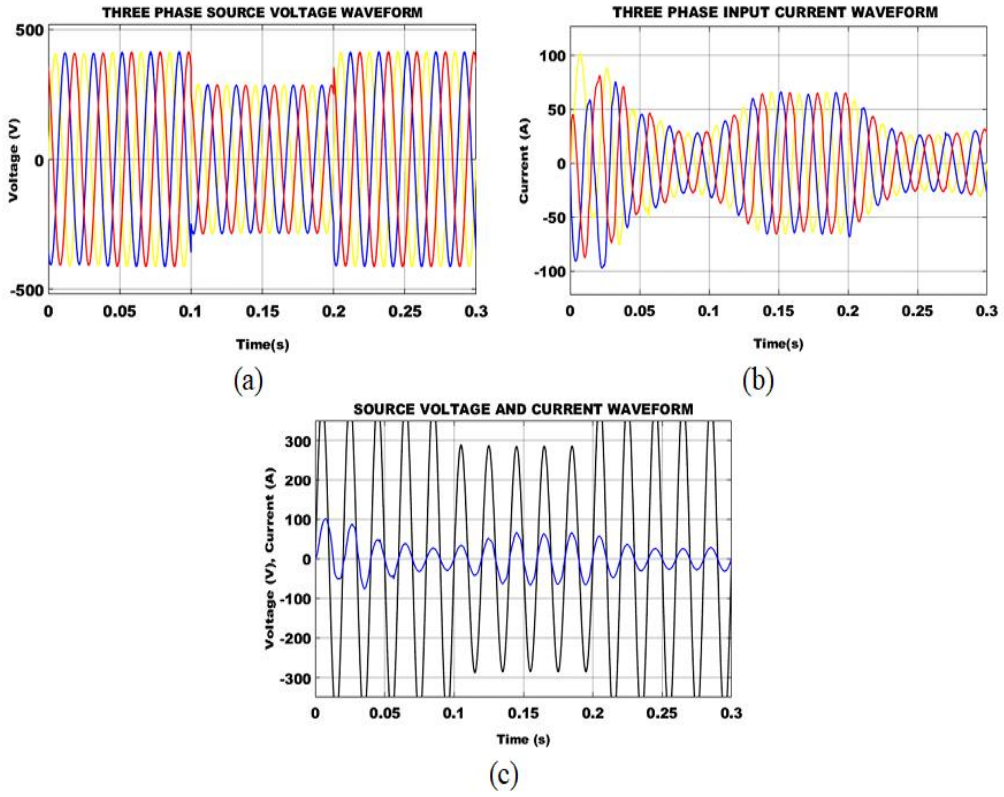

Figure 10: AC supply waveforms representing (a) Voltage (b) Current and (c) Combined Voltage and current

The waveforms representing the AC supplies voltage and current is given in *figure 10*. The magnitude of the AC voltage is 400V till 0.1s and then it dips to 280V till 0.2s. The voltage again recovers back to 400V from 0.2s. From the waveform, it is concluded that the source voltage is affected by the PQ issue of voltage sag of 120V from 0.1 to 0.2s. On observing *figure 10 (b)*, it is noted that the input current is not stable and it undergoes incessant variations.

FOREX Publication
Open Access | Rapid and quality publishing
International Journal of Electrical and Electronics Research (IJEER)
Research Article | Volume 11, Issue 1 | Pages 202-212 | e-ISSN: 2347-470X

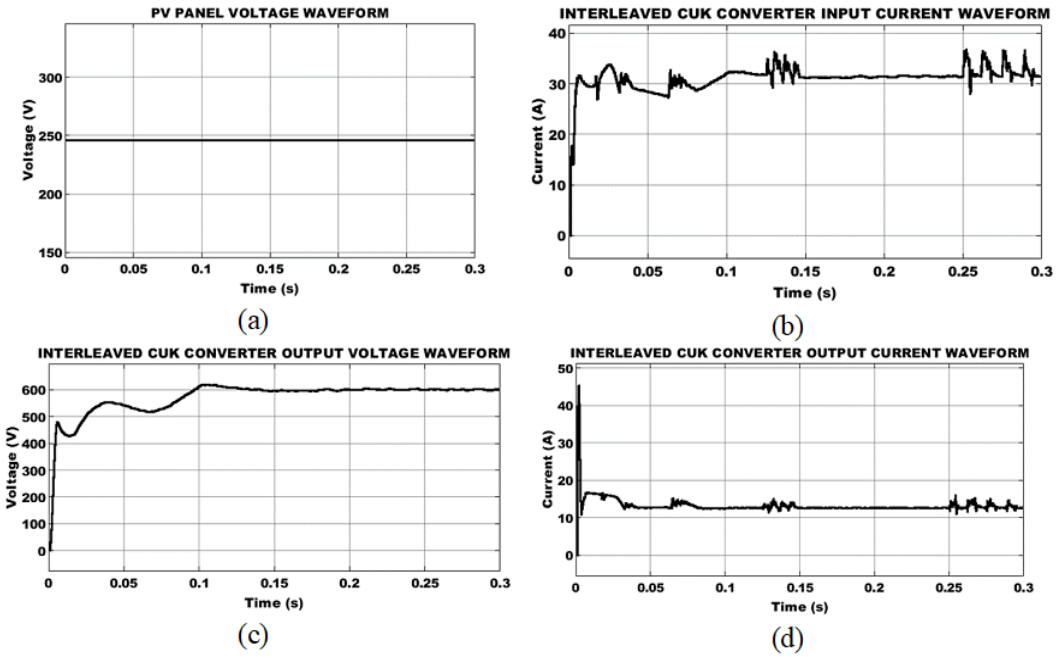

Figure 11: Interleaved Cuk-converter waveforms (a) Input voltage (b) Input current (c) Output Voltage and (d) Output current

An input voltage of 245 V is derived from the PV array as seen in *figure 11(a)* and it is provided to the Interleaved Cuk-converter. From *figure 11(b)*, it is noted that the PV output is not stable and affected by ceaseless fluctuations due to the influence of operating condition changes. A steady voltage of 600V is obtained from the Interleaved Cuk-converter from 0.15s with the aid of CSA assisted P&O MPPT. As indicated in *figure 11(d)*, an output current of 13A is obtained with minimum fluctuations. Thus, the proposed CSA assisted P&O MPPT in addition to Interleaved Cuk-converter is successful in improving the efficiency of PV.

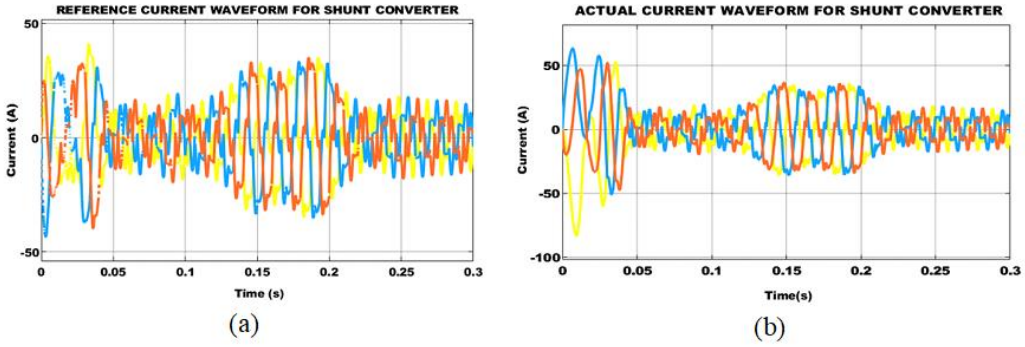

Figure 12: Shunt compensator waveforms (a) Reference current and (b) Actual current

The primal objective behind the implementation of a shunt converter is to compensate the load current harmonics. For eliminating the effect of current harmonics on the load side, a reference current of 30 A is generated from 0.15s to 0.2s as seen in *figure 12(a)*. As indicated in *figure 12(b)*, the series compensator also generates an actual current of magnitude 30A from 0.15s to 0.2s in accordance to the reference current.

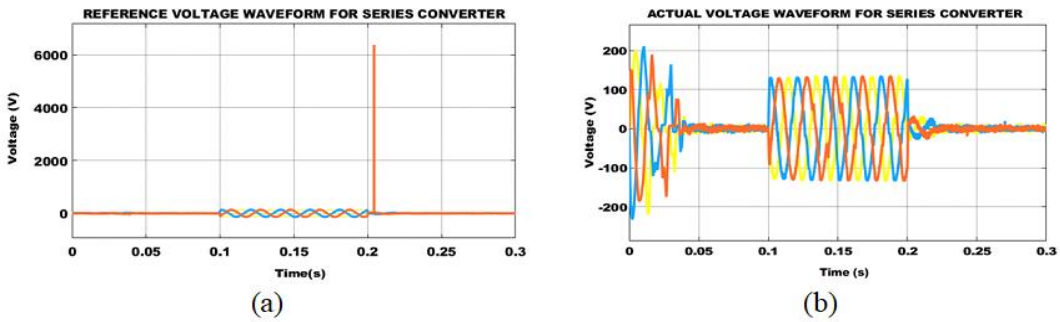

Figure 13: Series compensator waveforms (a) Reference voltage and (b) Actual voltage

FOREX Publication
Open Access | Rapid and quality publishing
International Journal of Electrical and Electronics Research (IJEER)
Research Article | Volume 11, Issue 1 | Pages 202-212 | e-ISSN: 2347-470X

The series compensator aims at stabilizing the source voltage through voltage sag compensation. The source voltage is affected by a voltage sag of magnitude 120V from 0.1 to 0.2s. In order to compensate this voltage sag, a reference voltage of 120V is set between 0.1 to 0.2s as seen in *figure 13 (a)*. Consequently, as seen in *figure 13(b)*, the series compensator generates a voltage of 120V from 0.1s to 0.2s for effectively stabilizing the source voltage.

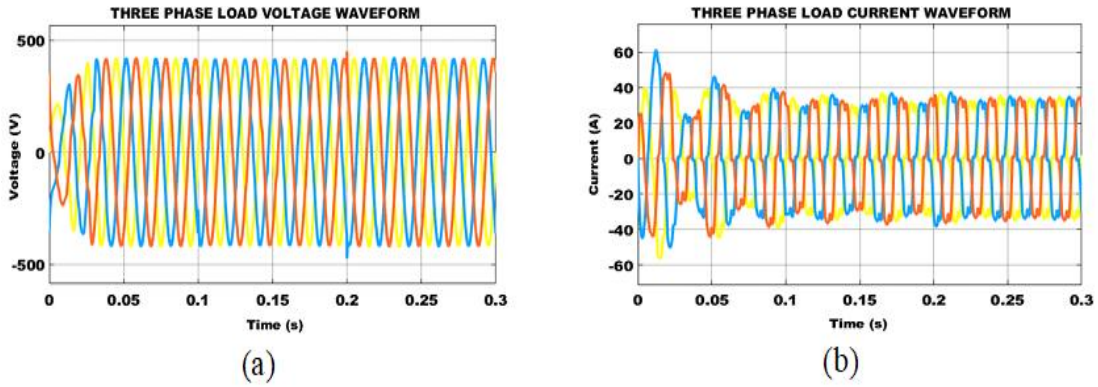

Figure 14: Waveforms representing (a) Load Voltage and (b) Load Current

Finally, a stable load voltage of magnitude 450V and steady current of magnitude 35A is obtained owing to the significance of the presented control technique. Thus, the designed configuration of PV-UPQC is effective in enhancing the PQ in both load and source side.

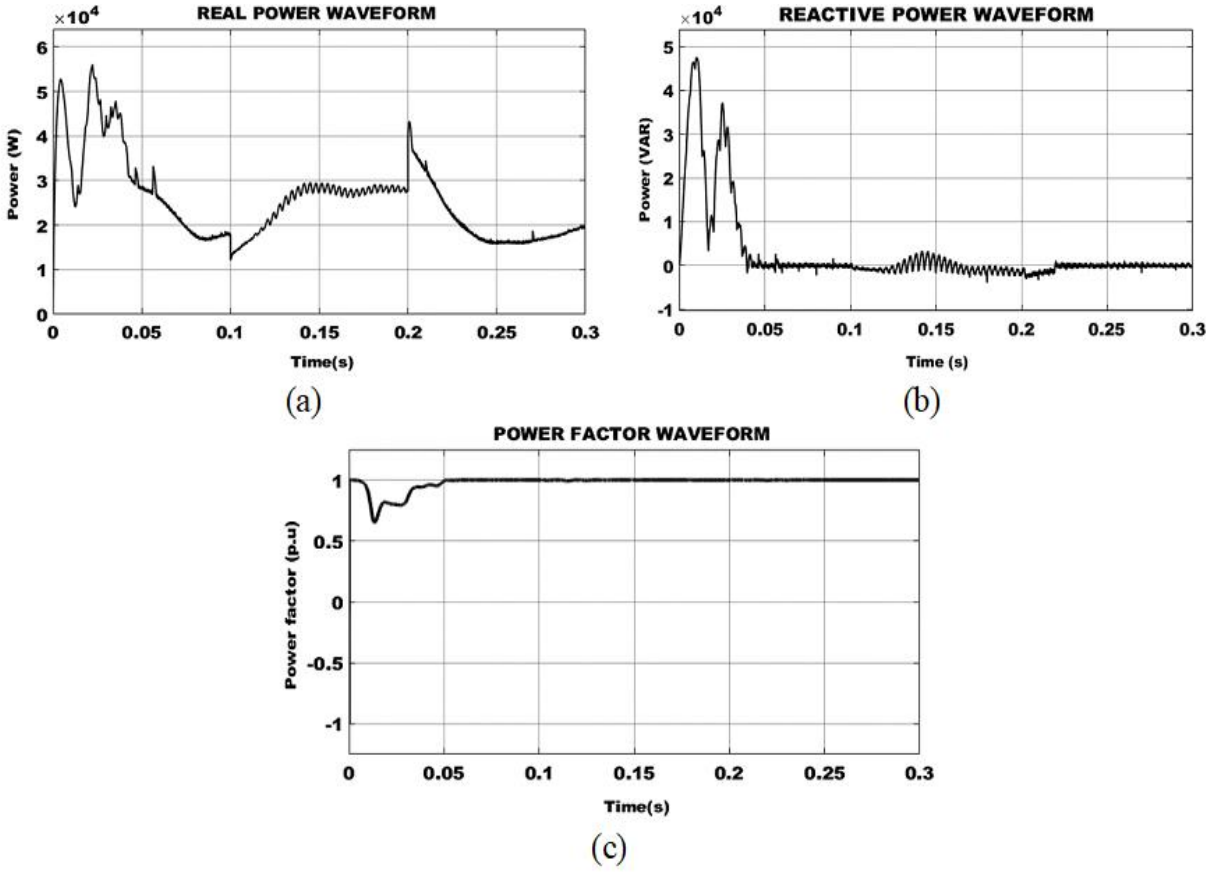

Figure 15: Waveforms representing (a) Real power (b) Reactive power and (c) Power factor

The waveforms representing the real power, reactive power and the power factor is displayed in *figure 15*. A power factor of value 1 is achieved from 0.05s, which proves that the PQ of the overall distribution system is improved by subduing the impact of current harmonics and voltage sag. As seen in *figure 16*, the value of THD is 3.25%.

FOREX Publication
Open Access | Rapid and quality publishing
International Journal of Electrical and Electronics Research (IJEER)
Research Article | Volume 11, Issue 1 | Pages 202-212 | e-ISSN: 2347-470X

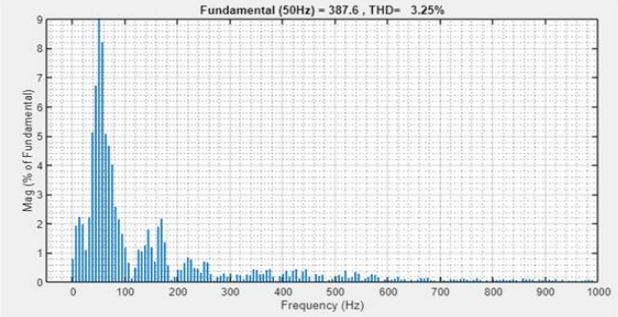

Figure 16: THD waveform

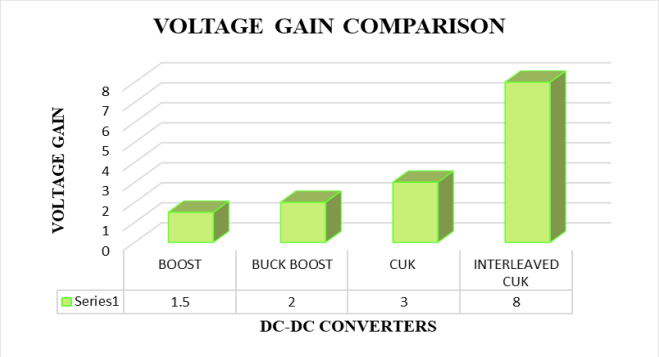

(a)

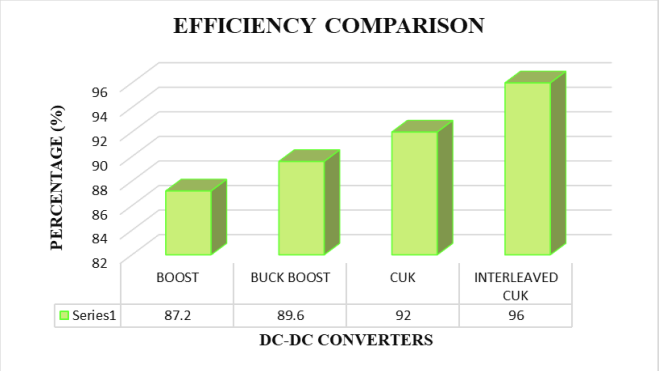

(b)

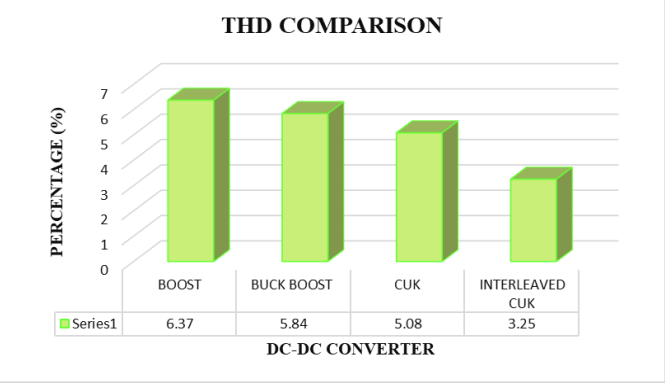

(c)

Figure 17: DC-DC converters performance comparison (a) Voltage gain (b) Efficiency and (c) THD

The operational performance of Interleaved Cuk-converter is analogized to several other available converters in terms of voltage gain, efficiency and THD as seen in Figure 17. The interleaved Cuk-converter operates with an excellent voltage gain and efficiency of values 1:8 and 96% respectively. Moreover, the THD of the Interleaved Cuk-converter is 3.25%, while the other converters have THD values greater than 5%, resulting in poor PQ.

5. CONCLUSION

The growing prevalence of sensitive power electronic devices has resulted in incurring various PQ issues in modern distributed power system. These issues if not addressed properly, have the potential to eventually lead to huge amount of economic loss due to overall system failure. Therefore, a PV-UPQC configuration, which enhances the PQ and promotes greener energy production is presented in this work. The PV being an intermediate power source leads to voltage instability if interfaced directly to the UPQC, so an Interleaved Cuk-converter is implemented for effective linking of PV to the UPQC. The Interleaved Cuk-converter comes with beneficial characteristic features such as ripple current elimination and continuous output and input current. Moreover, by adjusting the duty cycle of the Interleaved Cuk-converter, the power extraction from the PV array is maximized by the application of CSA assisted P&O MPPT. The designed hybrid MPPT technique operates exceptionally well under both PSC and uniform isolation conditions. According to the outcomes derived from MATLAB simulation, it is proved that the proposed PV-UPQC configuration is effective in improving the PQ of the load current and source voltage. The Interleaved Cuk-converter functions with an impressive efficiency of 96% along with a minimum THD of 3.25%.

REFERENCES

[1] S. Devassy and B. Singh, "Design and Performance Analysis of Three-Phase Solar PV Integrated UPQC," in IEEE Transactions on Industry Applications, vol. 54, no. 1, pp. 73-81, Jan.-Feb. 2018.

[2] E. Zangeneh Bighash, S. M. Sadeghzadeh, E. Ebrahimzadeh and F. Blaabjerg, "Adaptive-Harmonic Compensation in Residential Distribution Grid by Roof-Top PV Systems," in IEEE Journal of Emerging and Selected Topics in Power Electronics, vol. 6, no. 4, pp. 2098-2108, Dec. 2018.

[3] P. Shah and B. Singh, "Adaptive Observer Based Control for Rooftop Solar PV System," in IEEE Transactions on Power Electronics, vol. 35, no. 9, pp. 9402-9415, Sept. 2020.

[4] S. Devassy and B. Singh, "PLL-less d-q control of solar PV integrated UPQC," 2016 IEEE International Conference on Power Electronics, Drives and Energy Systems (PEDES), 2016.

[5] Adjustable Speed Drive Topology With Active Common-Mode Voltage Suppression," in IEEE Transactions on Power Electronics, vol. 30, no. 5, pp. 2828-2839, May 2015.

[6] A. Moghassemi, S. Padmanaban, V. K. Ramachandaramurthy, M. Mitolo and M. Benbouzid, "A Novel Solar Photovoltaic Fed TransZSI-DVR for Power Quality Improvement of Grid-Connected PV Systems," in IEEE Access, vol. 9, pp. 7263-7279, 2021.

[7] J. Ye and H. B. Gooi, "Phase Angle Control Based Three-phase DVR with Power Factor Correction at Point of Common Coupling," in Journal of Modern Power Systems and Clean Energy, vol. 8, no. 1, pp. 179-186, January 2020.

[8] C. Kumar, M. K. Mishra and S. Mekhilef, "A new voltage control strategy to improve performance of DSTATCOM in electric grid," in CES Transactions on Electrical Machines and Systems, vol. 4, no. 4, pp. 295-302, Dec. 2020.

International Journal of Electrical and Electronics Research (IJEER)
Research Article | Volume 11, Issue 1 | Pages 202-212 | e-ISSN: 2347-470X

[9] E. Lei, X. Yin, Z. Zhang and Y. Chen, "An Improved Transformer Winding Tap Injection DSTATCOM Topology for Medium-Voltage Reactive Power Compensation," in IEEE Transactions on Power Electronics, vol. 33, no. 3, pp. 2113-2126, March 2018.

[10] J. Yu, Y. Xu, Y. Li and Q. Liu, "An Inductive Hybrid UPQC for Power Quality Management in Premium-Power-Supply-Required Applications," in IEEE Access, vol. 8, pp. 113342-113354, 2020.

[11] P. Ray, P. K. Ray and S. K. Dash, "Power Quality Enhancement and Power Flow Analysis of a PV Integrated UPQC System in a Distribution Network," in IEEE Transactions on Industry Applications, vol. 58, no. 1, pp. 201-211, Jan.-Feb. 2022.

[12] M. Danbumrungtrakul, T. Saengsuwan and P. Srithorn, "Evaluation of DVR Capability Enhancement-Zero Active Power Tracking Technique," in IEEE Access, vol. 5, pp. 10285-10295, 2017.

[13] C. Kumar, M. K. Mishra and M. Liserre, "Design of External Inductor for Improving Performance of Voltage-Controlled DSTATCOM," in IEEE Transactions on Industrial Electronics, vol. 63, no. 8, pp. 4674-4682, 2016.

[14] F. Keyrouz, "Enhanced Bayesian Based MPPT Controller for PV Systems," in IEEE Power and Energy Technology Systems Journal, vol. 5, no. 1, pp. 11-17, 2018.

[15] K. Nathan, S. Ghosh, Y. Siwakoti and T. Long, "A New DC–DC Converter for Photovoltaic Systems: Coupled-Inductors Combined Cuk-SEPIC Converter," in IEEE Transactions on Energy Conversion, vol. 34, no. 1, pp. 191-201, 2019.

[16] M. Das, M. Pal and V. Agarwal, "Novel High Gain, High Efficiency DC–DC Converter Suitable for Solar PV Module Integration With Three-Phase Grid Tied Inverters," in IEEE Journal of Photovoltaics, vol. 9, no. 2, pp. 528-537, 2019.

[17] H. Renaudineau et al., "A PSO-Based Global MPPT Technique for Distributed PV Power Generation," in IEEE Transactions on Industrial Electronics, vol. 62, no. 2, pp. 1047-1058, Feb. 2015.

[18] D. A. Nugraha, K. L. Lian and Suwarno, "A Novel MPPT Method Based on Cuckoo Search Algorithm and Golden Section Search Algorithm for Partially Shaded PV System," in Canadian Journal of Electrical and Computer Engineering, vol. 42, no. 3, pp. 173-182, Summer 2019.

[19] P. Megantoro, Y. D. Nugroho, F. Anggara, Suhono and E. Y. Rusadi, "Simulation and Characterization of Genetic Algorithm Implemented on MPPT for PV System under Partial Shading Condition," 2018 3rd International Conference on Information Technology, Information System and Electrical Engineering (ICITISEE), 2018.

[20] Houam, Yehya, Amel Terki, and Noureddine Bouarroudj. "An efficient metaheuristic technique to control the maximum power point of a partially shaded photovoltaic system using crow search algorithm (csa)." Journal of Electrical Engineering & Technology 16, no. 1, 2021.

[21] Manikandan, M, P. Balakishan. and I. A. Chidambaram., Improvement of power quality in grid-connected hybrid system with power monitoring and control based on internet of things approach (July 20, 2022). Electrical Engineering & Electromechanics, (4), 44–50, 2022.

[22] M Manikandan, Sanepalle Gopal Reddy, S Ganapathy, ,2022 Three Phase Four Switch Inverter based DVR for power quality improvement with optimized CSA approach,IEEE Access, Institute of Electrical and Electronics Engineers (IEEE), 05 July 2022 10.1109/ACCESS.2022.3188629

[23] Manikandan, M, Praveen Kumar, T. and Ganapathy, S. and., Improvement of Voltage Stability for Grid Connected Solar Photovoltaic Systems Using Static Synchronous Compensator with Recurrent Neural Network (April 18, 2022). Electrical Engineering & Electromechanics, (2), 69–77, 2022. https://doi.org/10.20998/2074-272X.2022.2.10, Available at SSRN: https://ssrn.com/abstract=4091663

[24] Manikandan Sathish Ch, Chidambram I.A "Reactive Power Compensation in a Hybrid Renewable Energy System through Fuzzy Based Boost Converter" Problems of the Regional Energetics 2022, 1(53), DOI: https://doi.org/10.52254/1857-0070.2022.1-53.02(WOS-ESCI)-(Scopus)

[25] Manikandan M, Gopal Reddy S., Ganapathy S "Power quality improvement in distribution system based on dynamic voltage restorer using PI tuned fuzzy logic controller" Electrical Engineering & Electromechanics, 2022, no. 1, pp. 44-50. doi: https://doi.org/10.20998/2074-272X.2022.1.06

[26] M. Manikandan and Vishwaprakash Babu,2021 Power Quality Enhancement using Dynamic Voltage Restorer (DVR) Based Predictive Space Vector Transformation (PSVT) with Proportional Resonant (PR)-controller,IEEE Access, Institute of Electrical and Electronics Engineers (IEEE), 17 November 2021 DOI: 10.1109/ACCESS.2021.3129096

[27] Sachin B. Shahapure, Vandana A. Kulkarni (Deodhar), and Ramchandra P. Hasabe (2022), Performance Analysis of Renewable Integrated UPQC. IJEER 10(3), 508-517. DOI: 10.37391/IJEER.100318.

[28] Miska Prasad and A.K Akella (2022), Comparison of Voltage Swell Characteristics in Power Distribution System. IJEER 4(3), 67-73. DOI: 10.37391/IJEER.040302. http://ijeer.forexjournal.co.in/papers-pdf/ijeer-040302.pdf

[29] Himabindu Eluri, M. Gopichand Naik (2022), Energy Management System and Enhancement of Power Quality with Grid Integrated Micro-Grid using Fuzzy Logic Controller. IJEER 10(2), 256-263. DOI: 10.37391/IJEER.100234.